Chapter 1
Acoustic Characterization of Solid Periodic Ring Structures in Woodwind Musical Instruments

Alessandro Annessi, Alessia Caputo, Milena Martarelli, Daniele Eugenio Lucchetta, Davide Mencarelli, and Paolo Castellini

Abstract Woodwind musical instruments are a very interesting example of a vibro-acoustic device. They combine vibration, fluid dynamics and acoustics to create sound. While the basic concept of the instrument is, of course, well established, it is to this day possible to work on certain components for the purpose of improving, simply changing, certain characteristics of the instrument. Moreover, the interaction with the musician, who is in fact not only a performer but an integral part of the instrument, makes this analysis beyond challenging. In this paper, some innovative solutions will be analyzed by means of acoustic analysis with microphones and laser Doppler interferometry. The results obtained will be compared with numerical simulations in order to understand their behavior in depth.

Keywords Laser Doppler Vibrometry · Numerical Simulation · Periodic Structures · Musical Instruments · Acoustics

Introduction

Woodwind musical instruments offer a fascinating interplay of vibrational, fluid-dynamic, and acoustic behaviors that contribute to sound production. Despite a long history, there remains significant potential for research and innovation in improving and altering specific characteristics of these instruments. The interaction between the musician and the instrument further complicates this dynamic system, making it a rich field for both experimental and numerical study. In a wind instrument, regardless of the reed generation configuration, the motion of the vibrating reed valve is controlled by the pressure difference between the inlet and the outlet of the valve. The vibration frequency depends partly on the natural frequency of the reed and partly on the resonances of the air column of the instrument to which it is connected. The pressure difference across the valve is usually large enough that Bernoulli's equation can be applied. For a woodwind reed, the volume flow can then be expressed as [1]:

$$U = \alpha(p_0 - p)^{\frac{1}{2}} - \beta(p_0 - p)^{\frac{3}{2}} \tag{1}$$

where α and β are positive constants. This equation indicates that as the blowing pressure increases, the flow U rises from zero to a maximum value. Beyond this point, further increase in pressure causes the steady flow to decrease back to zero. Single reed instruments, such as the saxophone or clarinet, operate in the decreasing part of the curve where the conductance is negative and the reed acts as an acoustic generator. Starting from equation (1), it is straightforward to derive the pressure value p_c corresponding to the reed closing position (zero flow condition). The pressure corresponding to the maximum flow

Alessia Caputo · Milena Martarelli · Paolo Castellini
Department of Industrial Engineering and Mathematical Sciences, Polytechnic University of Marche, Ancona, Italy
e-mail: a.caputo@pm.univpm.it; m.martarelli@staff.univpm.it; p.castellini@staff.univpm.it

Alessandro Annessi
Department of Agricultural, Food and Environmental Sciences, Polytechnic University of Marche, Ancona, Italy
e-mail: a.annessi@staff.univpm.it

Daniele Eugenio Lucchetta
Optoacoustic Lab, SIMAU Department, Polytechnic University of Marche, Ancona, Italy
e-mail: d.lucchetta@staff.univpm.it

Davide Mencarelli
Department of Information Engineering, Polytechnic University of Marche, Ancona, Italy
e-mail: d.mencarelli@staff.univpm.it

Roland Platz et al. (eds.), *Model Validation and Uncertainty Quantification, Vol. 3*, Conference Proceedings of the Society for Experimental Mechanics Series, https://doi.org/10.13052/97887-438-0148-1_1

value is $p_a = \frac{1}{3}p_c$, and the player will use a pressure value between these points. Our goal is to determine the amplitude and shape of pressure and flow waveform fields under stationary conditions. Although the ideal lossless condition is a simplification, it serves as the best starting point for understanding the behavior of any single reed woodwind instrument, even when additional components that alter its acoustic properties are introduced. This study aims to introduce these additional components and examine their effects on the emitted sound spectra using an innovative experimental approach. The idea is to introduce solid periodic ring structures inside a small cylindrical volume to create sonic stop bands for selected frequencies. As a first step, before any practical application, we explored the possibility of attenuating the highest harmonic content of the input signal. In a clarinet, the highest note reaches 2 kHz, so our device should cut frequencies above 4 kHz to produce a mellow and pleasant sound, a strong requirement of classical musicians and the main motivation for our work. Recent advancements in 3D printing technologies have made it possible to fabricate periodic structures within the instrument's body. We tested several configurations through numerous simulations until we achieved promising results. Given the limited space inside the clarinet body, only a few ring element repetition (two or three) can be used. Limiting our choice to the simplest case of two elements, we found that rings with a triangular cross-section were more effective than other shapes. Varying a few geometrical parameters, such as the height of the ring, resulted in a significant change in the attenuation response. To accurately measure and analyze the impact of these modifications on sound production, advanced measurement techniques were required. One such technique is laser diffractive interferometry, which provides a powerful tool for investigating the fluid-dynamic and acoustic interactions within the instrument. In this study, a commercial Polytec Laser Doppler Vibrometer (LDV) with a Mach-Zehnder configuration was used. The LDV measures the Doppler frequency shift, which is proportional to changes in the laser optical path. Typically, LDV systems measure vibration velocities by detecting surface displacements. However, in this study, the Doppler signal results from the interaction between the laser and a turbulent flow, characterized by density fluctuations, which modifies the optical path, as the laser beam passes through it. Therefore, the measured signal is referred to as "pseudo-velocity". Changes in the optical path are due to variations in the refractive index, which change the wavelength of the laser as it travels through the turbulent region. The relationship between the refractive index and density fluctuations is crucial for interpreting the measured signal. Traditionally, the Gladstone-Dale relation is used to describe this relationship for fluid mixtures [2], but in this study, the more accurate Lorentz-Lorenz equation was considered [3, 4]. Temperature fluctuations can also affect the refractive index, however their contribution is considered negligible compared to pressure-induced variations, which dominate the measurement field [5]. This technique offers valuable insights into turbulent flow dynamics and acoustic wave interactions, both essential for understanding the behavior of complex systems such as musical instruments. By using such advanced methodologies, we can gain a deeper understanding of how modifications to the instrument, such as the introduction of periodic structures, influence the overall sound spectrum and performance. This provides a foundation for future innovations in instrument design and optimization.

The characterization of musical instruments, particularly woodwinds, has been extensively studied across various methodologies and technologies. These studies focus on the interactions between the player, the instrument, and the surrounding environment. A foundational reference in the study of woodwinds is provided by Fletcher et al., who explore the physical principles governing sound production, encompassing both theoretical and practical aspects [1]. Complementing this, Benade et al. examine the acoustical foundations of musical instruments, placing significant emphasis on the acoustic properties of woodwinds [6]. Wolfe et al. further investigate the interaction between the instrument and the player, modeling wind instruments as a combination of nonlinear elements (such as reeds or lips) alongside upstream and downstream ducts [7]. In addition, Lefebvre et al. present computational methods for analyzing woodwinds, including the Transmission-Matrix Method (TMM) for calculating input impedance and an optimization algorithm for determining tonehole positions and dimensions [8]. In addition, Lucchetta et al. apply Experimental Acoustic Modal Analysis (AMA) to a vintage tenor saxophone. This method measures Frequency Response Functions (FRFs) through acoustic pressure and volume velocity, identifying key modal parameters such as resonance frequencies and mode shapes. These insights enhance our understanding of the instrument's cavity modes and aid in validating analytical and numerical models [9]. Recent developments in laser-based techniques have provided new avenues for the non-invasive study of musical instruments. Bakarezos et al. explore the advantages of Electronic Speckle Pattern Interferometry (ESPI) for analyzing surface vibrations in instruments [10]. Huber et al. focus on scanning LDV for studying metal surface vibrations in guitars and organ reed pipes [11]. Beyond surface analysis, laser techniques are also used to study airflow and turbulence in woodwinds. Martarelli et al., Vanherzeele et al., and Castellini et al. highlight the use of LDV in detecting air fluctuations [12–15]. Mayrhofer et al., Woisetshlaeger et al. and Zipser et al. apply laser interferometry for frequency-resolved analysis of turbulent flows, further supported by uncertainty analysis from Castellini et al. [5, 16–19]. Additionally, Koeberl et al. and Kleine et al. demonstrate the effectiveness of interferometric techniques in visualizing compressible flows, contributing to a deeper understanding of air dynamics in woodwind instruments [20, 21]. These combined studies, ranging from traditional acoustic models to advanced optical measurements, provide a comprehensive framework for understanding and optimizing the acoustic performance of woodwind instruments.

Material and Methods

Solid periodic ring structure

The introduction of Solid Periodic Ring Structures (SPRS) inside a woodwind body represents a novel application. While the effects of periodic structures are well-understood in other domains, their impact on the emission properties of woodwind instruments has not yet been thoroughly investigated. To verify their effectiveness, we decided to use two simple configurations reported in Figure 1 which are compared to the unaltered ring-less SPRS reference. In the 2D case, the open lateral sides of each structure are sealed using a glass slide in order to avoid any pressure leak and, at the same time, allow the probe laser light to pass through the elements. The aim is to achieve an alteration of the instrument's timbre in a very high-frequency range, in such a way as to cut off the sharpest components and give the sound with a greater sense of roundness, enhancing its suitability for inclusion in classical performances. The distance d between periodic rings should only affect the highest harmonic content of the sound spectra.

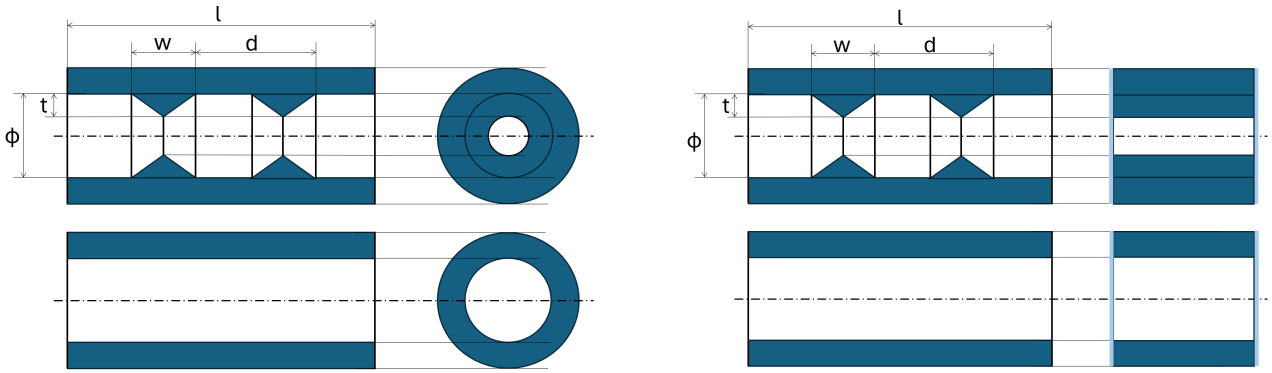

(a) Axisymmetric (b) 2D

Fig. 1 Illustration of the two SPRS tested in the study. The left image (a) shows the axisymmetric (circular) configuration, while the right image (b) displays the 2D (square) configuration

In view of future optimizations, as a first attempt, we decided to vary the height t of the rings by 1 mm by leaving unaltered the other parameters, obtaining two configurations referred to as wide and narrow rings. Those configurations are then compared to a stucture having flat walls (no rings) considered as a reference. Geometrical parameters are reported in Table 1. The above mentioned structure were designed in the Rhinoceros™ CAD environment and 3D printed using a 405nm LCD commercial printer.

Table 1 Dimensions of the three 3D printed structures under test.

	t [mm]	w [mm]	d [mm]	l [mm]	Φ [mm]
Flat walls	0	0	0	75	15
Wide Rings	4	16	25	75	15
Narrow Rings	5	16	25	75	15

Experimental set-up

The experimental analysis was conducted using a Polytec PSV-500 Scanning Laser Doppler Vibrometer (LDV) which is focused onto a fixed surface, a B&K microphone (model 378 B02 PCB, 1/2 inch) aligned to the nozzle axis to capture the acoustic field from the instrument under test and a monopole volume acceleration source (Simcenter Qsources Mid-Hig Frequency Volume Source, model Q-MHF) with an internal reference sensor connected to the SPRS as excitation. The experimental setup aimed to evaluate the acoustic pressure fluctuations and corresponding density variations within and around the SPRS introduced inside the instrument. The entire experimental setup, including the positioning of the LDV and microphone, is illustrated in Figure 2. The LDV system was configured to capture density fluctuations in the air caused by vibrating air column within the instrument. This is achieved by pointing the laser at a non-vibrating co-operative surface,

specifically a rigid wall covered by reflecting tape, with the sole function of reflecting as much light back as possible. Air density fluctuations directly affect the optical path of the laser beam, making it possible to map the dynamic behavior of the instrument's internal acoustics. The LDV captures pseudo-velocity by measuring the Doppler frequency shift, which corresponds to the changes in the optical path length due to the density variations in the vibrating air. The microphone was placed at a distance of 42 cm from the jet outlet in the near field, slightly downstream, to avoid interference with the airflow while maintaining a high Signal-to-Noise Ratio (SNR). A grid of measurement points was defined inside the SPRS section in the surrounding area to ensure a statistically valid dataset. Each point on this grid was scanned using the LDV to acquire pseudo-velocity data. The spectral bandwidth was set to 12.5 Hz – 10 kHz, with a spectral resolution of 12.5 Hz across 800 spectral lines. The sampling frequency was 25 kHz. A Hanning window was set for the acquisition to avoid leakage related issues. Moreover, each grid point measurement was averaged 16 times to enhance SNR. The excitation signal, which is a white noise, was provided using the built-in Polytec signal generator. The total number of measurement points varied depending on the specific sample under examination. For the cylindrical sample, 3479 points were measured, while for the prismatic sample, 3305 points were recorded. The wide rings and narrow rings samples were measured with 3262 and 3251 points respectively. Notably, only the grid corresponding to the cylindrical sample with flat walls (no rings) is rectangular, comprising 49 elements in the Y direction and 71 elements in the X direction. In contrast, the grids for the other samples have been custom-designed to meet specific experimental requirements. The primary goal for the experimental campaign was to compare the external acoustic pressure measured by the microphone with the internal pseudo-velocity data gathered by the LDV, allowing for a comprehensive evaluation of the interaction between the instrument's structural modifications and the corresponding acoustic field.

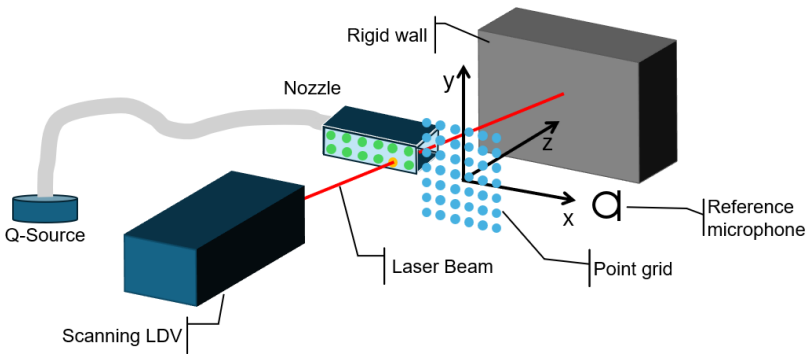

Fig. 2 Overview of the experimental set-up for the microphone and vibrometry measurements

Numerical Simulations

Numerical simulations are carried out by means of COMSOL Multiphysics Pressure Acoustic module, specific for modelling the propagation of sound waves through fluids. It operates in the frequency domain, allowing for the analysis of harmonic pressure variations in applications involving stationary fluids, like in the present case. Specifically, the sound pressure represents the deviation of the instantaneous pressure from the ambient atmospheric pressure, assuming a static fluid environment without significant flow.

Axisymmetric simplifying condition is assumed in the simulations: both geometry and boundary conditions approximately exhibit rotational invariance, and their analysis can be reduced to a 2D cross-sectional study.

Three types of boundary conditions are needed to characterize the device physics:

- Spherical radiation boundaries are imposed at the outer surface of the computational domain, assumed to be a sphere much larger than the device under test (DUT). In this way, a spherical-wave approximation is implied on the above boundaries: outgoing spherical sound waves can pass through the boundary without significant reflections. The only small discontinuity in the radiation boundary is given by the acoustic cylindrical waveguide carrying the acoustic power, but such perturbation occurs at large distance from the DUT, and, as a matter of fact, a negligible fraction of the injected acoustic power is radiated backward.
- Solid, reflective surfaces are assumed on the surface of the woodwind instrument: normal component of sound waves are prevented from penetrating the device as if encountering a rigid, unyielding wall.

- Wave-port condition is used to simulate the incident pressure field having the form of an acoustic wave injected into the feeding waveguide. The incident pressure field constitutes the input excitation of the problem and assumes the simple form of a plane-wave owing to its spatial uniformity in the section of the waveguide.

It is remarked that the wave-port is considered as transparent, meaning that waves possibly reflected back to it are perfectly absorbed. Such condition is satisfied, in case of plane-wave "radiation option", if the reflected waves propagate near the normal to the port. Otherwise, rigorous multimode analysis is needed at the port, or at least, a proper perfectly-matched-layer (PML) setup. Such issue is not affecting significantly the present simulation, as, in fact, the waveguide section is smaller than typical acoustic wavelengths, and the transverse profile of the acoustic field is highly constrained.
The acoustic pressure level is provided by the numerical solver throughout the computational domain. The acoustic pressure level, sampled at a point along the axis of the axisymmetric domain and located 40 cm from the woodwind instrument, is analyzed to illustrate the harmonic pressure variations within the system.

Results

This section details the results of acoustic measurements conducted on various configurations of the SPRS. Each measurement type offers critical insights into how structural modifications influence the acoustic properties and behavior of the SPRS, thereby providing a thorough understanding of its performance under varying conditions.
Figure 3 illustrates the comparison of acoustic pressure levels across three configurations: flat walls (no rings), narrow rings, and wide rings. Each curve is normalized for clarity, allowing for a direct comparison of the acoustic responses. The results demonstrate how the presence and geometry of the rings significantly impact the acoustic response of the system.

- Flat walls (No Rings): The baseline configuration exhibits a broad frequency response, with relatively high levels of acoustic pressure across a wide range of frequencies. This indicates that the absence of structural modifications leads to less targeted wave interaction.

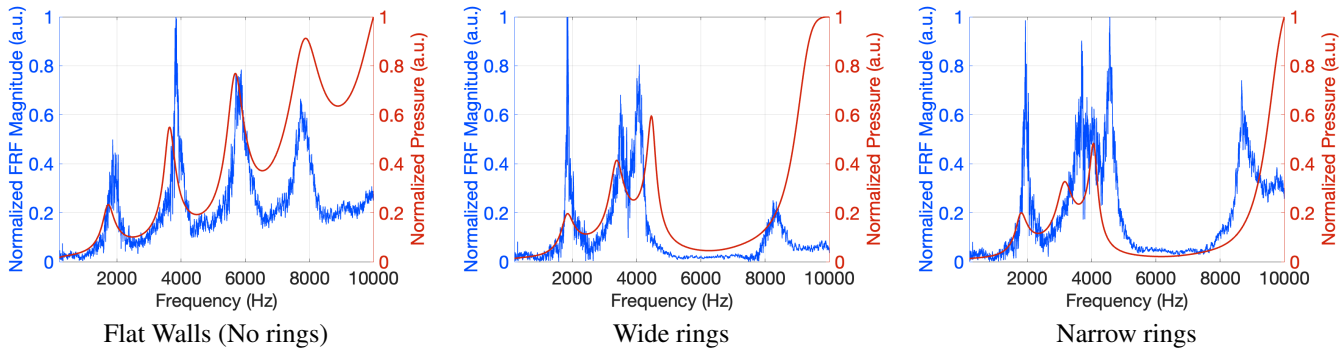

Fig. 3 Comparison of acoustic pressure levels across three configurations: flat walls (no rings), wide rings and narrow rings (numerical data in red, experimental data in blue)

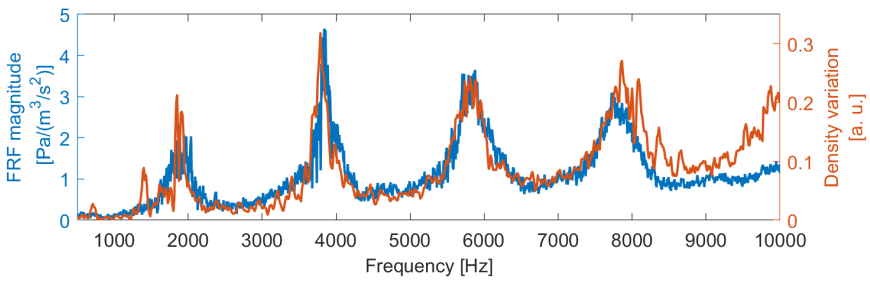

Fig. 4 Comparison between the acoustic FRF measured by the microphone and the density variation measured by the LDV for the element with flat walls (no rings).

- Narrow Rings: The introduction of narrow rings in the geometry alters the frequency response, creating specific resonances that affect the amplitude of the acoustic pressure. These resonances appear as distinct peaks in the spectrum, showcasing how the geometry influences sound behavior.
- Wide Rings: The presence of wide rings produces a different frequency response compared to the narrow rings. The wider geometry shifts the frequency characteristics further, demonstrating a more pronounced impact on the high-frequency content of the acoustic signal.

The comparison between microphone and LDV measurements is shown in Figure 4. Microphone measurements provides data on the external acoustic pressure, reflecting how sound propagates beyond the instrument. LDV measurements capture density variations associated with the acoustic wave. The resulting spectra reveal how these density changes correlate with the sound pressure levels measured by the microphone.

Figure 5 shows a representative example of the amplitude and phase map for the prismatic attenuator configuration (flat walls condition) at a frequency of 7.6 kHz. These maps serve as a reference point to evaluate the influence of the absence of rings on the acoustic behavior of the system.

Finally, in Figure 6, the numerical and experimental phase maps (color scale ranging from $-\frac{\pi}{2}$ to $\frac{\pi}{2}$) for the three configurations (no rings, wide rings and narrow rings) are compared at the fourth resonance frequency. Concerning the numerical model for the wide and narrow rings configurations, the phase maps reveal that nodal lines align with the constrictions, where a node emerges along the symmetry axis. This suggests that, at the frequency in question, sound waves concentrate around these areas due to the geometric changes, with waves being partially reflected and refracted at the constrictions. This behavior contrasts with the flat walls configuration (no rings), where the absence of physical obstructions causes the nodal lines to distribute differently. The experimental results follow a similar trend however exhibiting some discrepancies, which are primarily attributable to the 3D printing process. In fact, its accuracy is not sufficient to produce flawless constrictions in terms of geometry and roughness in the specimens, as in the numerical model. These irregularities affect the sound wave

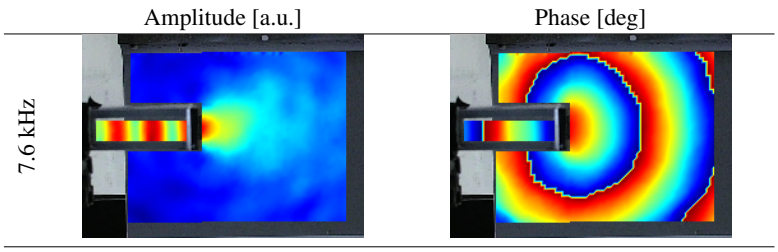

Fig. 5 Amplitude and phase maps for the prismatic attenuator configuration at the fourth resonance frequency (7.6 kHz).

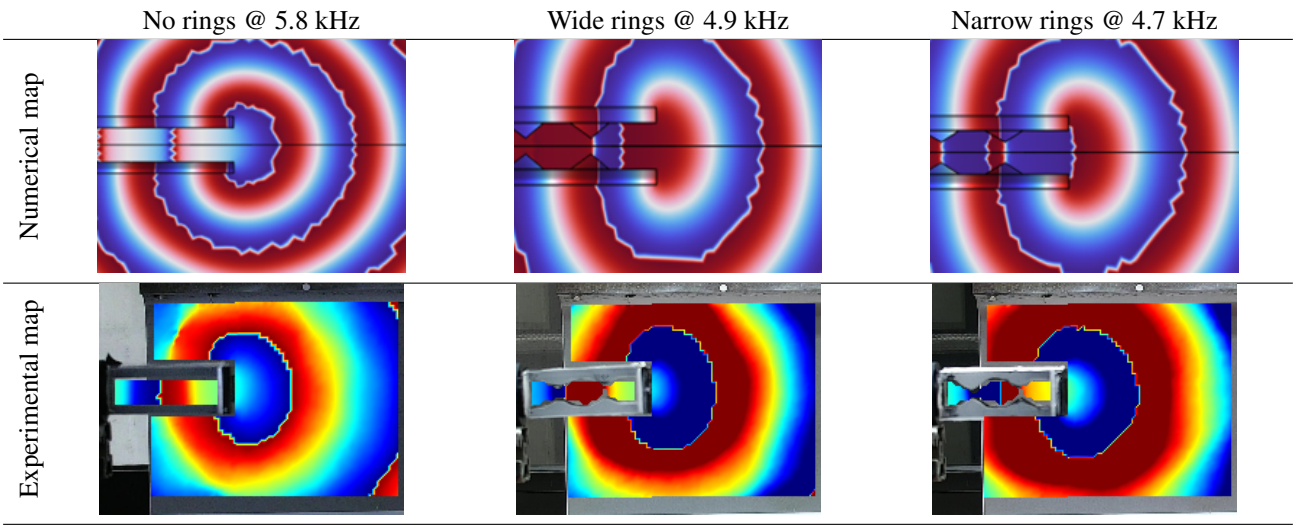

Fig. 6 Comparison between phase maps for wave propagation in the flat walls (no rings), wide rings and narrow rings structures calculated from the numerical model and experimentally measured.

propagation and the formation of nodal lines. Additionally, the acoustic pressure measurements are subjected to uncertainties caused by density fluctuations due to external factors, setup assembly and geometric imperfections of the specimen under test.

Conclusion

This study investigated the effects of Solid Periodic Ring Structures (SPRS) introduction on the acoustic properties of woodwind instruments. Different geometrical configurations of periodic rings are explored evaluating their impact on the sound spectra and overall acoustic behavior. Both numerical predictions and experimental results highlighted the crucial influence of rings presence on the acoustic pressure levels and frequency response of the instruments. Moreover, their design significantly affects the acoustic response. The configurations with narrow and wide rings produced distinct resonances, leading to targeted modifications of the sound output. This results suggest that a careful design of ring geometry can enhance the quality of sound by attenuating undesirable harmonics, thereby aligning the instrument timbre with the preferences of classical musicians seeking a mellow tone. The correlation between external acoustic pressure and internal density variations, measured with a microphone and a LDV respectively, underscores the importance of understanding these interactions to optimize instrument design. Furthermore, the numerical simulations corroborated the experimental findings, illustrating the nodal patterns in sound wave propagation influenced by the SPRS. Although discrepancies were noted due to the limitations of the 3D printing process, the alignment of nodal lines with structural modifications affirms the potential of using numerical models to predict acoustic behaviors effectively. Future research should focus on refining the manufacturing process of the SPRS to enhance structural accuracy and improve acoustic consistency. Exploring additional configurations and materials for the periodic structures could further optimize sound characteristics.

Acknowledgments This research has received funding from the project *Sustainable Mobility Center* – Project Code CN00000023, CUP I33C22001240001 - funded under the National Recovery and Resilience Plan (NRRP), Mission 4 Component 2 Investment 1.4 - Enhancement of research structures and establishment of "national champions" in R&D on selected Key Enabling Technologies "Sustainable Mobility Center (Centro Nazionale per la Mobilità Sostenibile – CNMS)" Call for tender No. 3138 of 16/12/2021, and Concession Decree No. 0001033.17-06-2022 of the Italian Ministry of University funded by the European Union – NextGenerationEU.

References

1. Fletcher, N.H. and Rossing, T.D. *The Physics of Musical Instruments*. Springer New York (1998)
2. Merzkirch, V.W. "Flow visualization". *Chemie Ingenieur Technik*, 48(12):1224–1224 (1976)
3. H.Lorentz. "Ueber die beziehung zwischen der fortpflanzungsgeschwindigkeit des lichtes und der körperdichte". *Wied. Annuals of Physics*, 9(641) (1880)
4. Lorenz, L. "Beiträge zur optik trüber medien, speziell kolloidaler metallosurcgem". *Wied. Annuas Physics*, 11(7) (1880)
5. Castellini, P. and Martarelli, M. "Uncertainty analysis of hybrid numerical-experimental procedures: Application to flow density measurements". In *Conference and Exposition on Structural Dynamics 2006, IMAC-XXIV* (2006)
6. Benade, A.H. *Fundamentals of musical acoustics*. Dover books on music, music history. Dover Publ., New York, NY, 2nd, rev. ed. edition (1990) Unabridged, extensively corrected republication of the edition originally published by Oxford University Press in 1976.
7. Wolfe, J., Chen, J.M., and Smith, J. "The acoustics of wind instruments - and of the musicians who play them". In *20th International Congress on Acoustics*, volume 5, page 4061–4070 (2010)
8. Lefebvre, A. *Computational acoustic methods for the design of woodwind instruments*. PhD thesis, Computational Acoustic Modeling Laboratory, McGill UniversityMontreal, Quebec, Canada (2010)
9. Lucchetta, D.E., Schiaroli, L., Battista, G., Martarelli, M., and Castellini, P. "Experimental acoustic modal analysis of a tenor saxophone". *The Journal of the Acoustical Society of America*, 152(5):2629–2640 (2022)
10. Bakarezos, E., Orphanos, Y., Kaselouris, E., Dimitriou, V., Tatarakis, M., and Papadogiannis, N.A. *Laser-Based Interferometric Techniques for the Study of Musical Instruments*, pages 251–268. Springer International Publishing (2019)
11. Huber, T.M. "Measurement of mode shapes of musical instruments using a scanning Laser Doppler vibrometer". *The Journal of the Acoustical Society of America*, 129(4Supplement):2615–2615 (2011)
12. Martarelli, M., Castellini, P., and Tomasini, E.P. "Subsonic jet pressure fluctuation characterization by tomographic Laser interferometry". *Experiments in Fluids*, 54(12) (2013)
13. Martarelli, M., Castellini, P., and Tomasini, E.P. "Aeroacoustic model for the prediction of turbulent free jets noise using scanning Laser Doppler vibrometry". In *Conference and Exposition on Structural Dynamics 2005, IMAC-XXIII* (2005)
14. Vanherzeele, J., Brouns, M., Castellini, P., Guillaume, P., Martarelli, M., Ragni, D., Primo Tomasini, E., and Vanlanduit, S. "Flow characterization using a Laser Doppler vibrometer". *Optics and Lasers in Engineering*, 45(1):19–26 (2007)
15. Castellini, P. and Martarelli, M. "Aeroacoustic characterization of turbulent free jets using scanning Laser Doppler vibrometry". In *Sixth International Conference on Vibration Measurements by Laser Techniques: Advances and Applications*. SPIE (2004)

16. Mayrhofer, N. and Woisetschläger, J. “Frequency analysis of turbulent compressible flows by Laser vibrometry”. *Experiments in Fluids*, 31(2):153–161 (2001)
17. Woisetschläger, J., Mayrhofer, N., Hampel, B., Lang, H., and Sanz, W. “Laser-optical investigation of turbine wake flow”. *Experiments in Fluids*, 34(3):371–378 (2003)
18. Zipser, L. and Franke, H. “Visualization and measurement of acoustic and fluidic phenomena using a Laser scanning vibrometer”. In Tomasini, E.P., editor, *Fifth International Conference on Vibration Measurements by Laser Techniques: Advances and Applications*. SPIE (2002)
19. Castellini, P. and Martarelli, M. “Flow pressure fluctuation measurement by means of interferometric technique combined with tomographic reconstruction”. In *38th International Congress and Exposition on Noise Control Engineering, INTER-NOISE* (2009)
20. Kleine, H., Grönig, H., and Takayama, K. “Simultaneous shadow, schlieren and interferometric visualization of compressible flows”. *Optics and Lasers in Engineering*, 44(3–4):170–189 (2006)
21. Köberl, S., Fontaneto, F., Giuliani, F., and Woisetschläger, J. “Frequency-resolved interferometric measurement of local density fluctuations for turbulent combustion analysis”. *Measurement Science and Technology*, 21(3):035302 (2010)